

LA-7989

3

CIC-14 REPORT COLLECTION

REPRODUCTION  
COPY

**Numerical Modeling of Sympathetic Detonation**

University of California



**LOS ALAMOS SCIENTIFIC LABORATORY**  
Post Office Box 1663 Los Alamos, New Mexico 87545

**An Affirmative Action/Equal Opportunity Employer**

This work was supported by the US Department of Energy, Office of Military Application, and the US Department of the Navy, Strategic Systems Project Office.

This report was prepared as an account of work sponsored by the United States Government. Neither the United States nor the United States Department of Energy, nor any of their employees, nor any of their contractors, subcontractors, or their employees, makes any warranty, express or implied, or assumes any legal liability or responsibility for the accuracy, completeness, or usefulness of any information, apparatus, product, or process disclosed, or represents that its use would not infringe privately owned rights.

LA-7989

UC-45

Issued: November 1979

# Numerical Modeling of Sympathetic Detonation

Allen L. Bowman  
James D. Kershner  
Charles L. Mader



# NUMERICAL MODELING OF SYMPATHETIC DETONATION

by

Allen L. Bowman, James D. Kershner, and Charles L. Mader

## ABSTRACT

The sympathetic detonation of small cubes of solid rocket propellant was modeled numerically, using the Eulerian reactive hydrodynamic code 2DE with Forest Fire burn rates. The model was applied to cubes of 1-3 in., with excellent agreement between calculated and experimental results. The model also was applied to several propellants and to different experimental arrangements. The blast-wave pressures in the air gap and the induced shock pressures in the acceptor were obtained from the model. The correlation between these pressures was coupled with a study of the effect of the length-to-diameter ratio of a donor cylinder and the necessary conditions for detonation of the acceptor to provide a semiquantitative predictive capability.

---

## I. INTRODUCTION

A major problem in the handling and storage of munitions, and of explosive materials in general, is sympathetic detonation, which is the detonation of nearby explosive objects by the blast or debris from a primary explosion. Concern with the problem of sympathetic detonation has increased with the coming of rocketry and the high-impulse solid fuels that are being developed for propellants. These fuels are composed mainly of explosive substances.

Critical separation distances are needed to prevent the propagation of an explosive reaction from one motor to another. Another problem is the possibility of the propagation of an impact-initiated detonation through a series of propellant fragments in a damaged motor resulting in the detonation of the remaining propellant grain.

Hercules, Inc., and the Thiokol Corp. have performed an extensive experimental study of the sympathetic detonation of selected rocket propellants under the cognomen "A Joint Venture." They have studied the effects of size, shape, damage, method of initiation, and other variables. We at the Los Alamos Scientific Laboratory are modeling the sympathetic detonation experiments numerically to provide a better understanding of the details of the process and a means for predicting results of future tests.

## II. EXPERIMENT AND MODEL

The numerical study of sympathetic detonation has been directed primarily toward a single test. This test involves two 2-in. cubes of VRO propellant mounted as shown in Fig. 1. The cube

within which a detonation is first initiated is defined as the donor cube. The other cube, which is assumed to be affected by the detonation of the donor cube, is called the acceptor cube. The donor cube is backed by a steel plate, and is initiated by a J-2 cap inserted through a hole in the plate. The extent of reaction of the acceptor cube is determined by the effect on a lead witness cylinder. Typical postexperiment witness cylinders that illustrate such effects are shown in Fig. 2. The experimental arrangement is shown in Fig. 3.

The computation of sympathetic detonation behavior was performed with the two-dimensional Eulerian reactive hydrodynamic code 2DE<sup>1,2</sup> using the Forest Fire burn rate.<sup>2,8</sup> The equation-of-state data used in these calculations are given in App. A. The Forest Fire burn rate parameters and Pop plot data are given in App. B. The 2-in. cubes of the experiment were modeled by equivalent cylinders, 2.8678 cm in radius and 5.0738 cm long, with a 0.002% difference in volume and a 0.1% difference in surface area of the matched faces. Calculations for the experimental cubes were made with these equivalent cylinders. The model geometry is shown in Fig. 4. The cap initiation was modeled by an initial hot spot of 0.8824 cm in radius and length.

The same model was used for experiments with 1- and 3-in. cubes. It was also used without the steel backing to determine the effect of the plate. The effect of impact initiation of the donor cube was studied by eliminating the hot spot and giving the plate or the donor cube an initial velocity. The flying plate experiment was modeled by giving the plate an initial velocity. The donor cube was given an initial velocity in an end-on approximation of the actual shotgun-type experiment in which the acceptor sample is located to the side.

### III. RESULTS AND DISCUSSION

The detonation behavior of a VRO donor cylinder is shown in Fig. 5 by a series of contour plots of mass fraction, pressure, and density. The mass fraction  $W$  is defined such that  $W = 1$  for a solid and  $W = 0$  for a gas, with a continuous variation between these limits for a burning propellant. The calculated detonation pressure in the donor cylinder is steady at approximately 28 GPa, in good agreement with the C-J pressure of 29.2 GPa obtained from a BKW calculation.<sup>4</sup> The progress of the blast wave through the air gap and of the shock wave in the acceptor cylinder is shown by isopycnic plots in Fig. 6. The initiation and propagation of a detonation in the acceptor cylinder are shown by mass fraction contour plots in Fig. 7.

These figures describe the results of the calculation for simulated 2-in. cubes of VRO with a separation distance of 3.1 cm, but the general features of Figs. 5 and 6 are repeated in all calculations, with change of magnitude only. The length of run to detonation, which appears in Fig. 7 as the distance from the face of the cylinder to the first point of complete reaction ( $W = 0$ ), increases with increasing separation distance to an abrupt transition to a very limited reaction ( $W > 0.9$ ).

The critical separation distance is defined as the midpoint between the longest gap for which detonation occurs and the shortest gap for which no detonation occurs. It appears from comparison with experimental results that the critical separation distance represents the observed transition from high-order detonation to a low-order detonation. Thus, a very significant reaction can be induced by a shock that is too weak to produce a direct shock-initiated detonation. This phenomenon cannot be described by our present numerical model.

The most complete calculations have been carried out on simulated 2-in. cubes of VRO. These include the basic experiment and numerical studies of the effect of removing the steel backing plate and of impact initiation of the donor cylinder against a steel plate. The calculated critical separation distances for various conditions are compared in Table I. The effect of cube size on the critical separation distance was studied with simulated 1-, 2-, and 3-in. cubes of VRO. The calculated values are compared with experimental results in Fig. 8. Note that extrapolation of the fitted straight line in Fig. 8 to 8-in. cubes gives a predicted critical separation distance of

TABLE I

## CRITICAL SEPARATION DISTANCE

	<u>cm</u>
Cap Initiation 1.3-cm steel backing plate	3.64
Cap Initiation No support plate	3.42
Impact Initiation Flying steel plate (1.3 cm) ( $V_o = 0.1 \text{ cm}/\mu\text{s}$ ) <sup>a</sup>	4.08
Impact Initiation Shotgun against steel ( $V_o = 0.1 \text{ cm}/\mu\text{s}$ ) <sup>a</sup>	2.98

<sup>a</sup>The velocity at impact of the flying plate on the shotgun sample is  $V_o$ .

TABLE II

## CRITICAL SEPARATION DISTANCE

<u>Propellant</u>	<u>Calculated (in.)</u>	<u>Experimental (in.)</u>
VOP-7	$2.8 \pm 0.9^a$	---
VRO	$1.4 \pm 0.1^a$	1.0 - 1.5
VRP	$1.2 \pm 0.2^a$	0.5 - 1.0
VTQ-2	$2.6 \pm 0.2^a$	---

<sup>a</sup>The uncertainty in the calculated distance is one-half the distance between calculated go and no-go separation distances.

17.02 cm, whereas a high-order detonation has been observed experimentally at 30.48 cm. Thus, one must be careful when extending these results to significantly larger samples. The calculated critical separation distances for simulated 2-in. cubes of several different propellants are shown in Table II.

The shock pressures that are induced in the acceptor cube are determined by performing the calculation with no decomposition reaction allowed in the acceptor. The shock pressures along the cylindrical axis are shown in Fig. 9 for a simulated 2-in. cube of VRO with a 3.2-cm gap. The maximum induced pressures in VRO are shown in Fig. 10 as a function of separation distance for different size cubes. The data points are fitted to a curve of the form  $p = Ax^{-n}$ .

The calculated shock pressures and lengths of run to detonation show very good agreement with the Pop plot for VRO. (See Fig. 17.) The run distance at the critical separation distance, obtained from the induced pressure curves of Fig. 10 and the Pop plot, is approximately 0.75 times the cylindrical radius of the simulated cube.

The blast pressures that are developed in the air gap are shown in Fig. 11 for the three VRO cube sizes of this study. They are the pressures calculated along the cylinder axis of the simulated cubes. These pressures are found to scale with the cube root of the mass. The air shock wave decays quickly to approximately 0.01 GPa, and then decays more slowly. It is followed by the much stronger detonation products shock wave, which is clearly the cause of the direct shock-initiated detonation. The observed shock pressures at the critical separation distance are summarized in Table III. The variation of the peak blast pressure with separation distance is shown in Fig. 12.

The maximum shock pressure in the acceptor is found to be related to the peak blast pressure by the equation

$$p_I = 11.75 p_B^{2/3},$$

**TABLE III**  
**SYMPATHETIC DETONATION OF VRO**

Cube Size (in.)	<u>1</u>	<u>2</u>	<u>3</u>
Critical Separation Distance (mm)	12.7	36.4	57.9
Induced Shock Pressure <sup>a</sup> (GPa)	4.98	3.64	3.44
Run Length (from Pop plot) (mm)	10.9	23.3	26.8
Run Length/Radius	0.76	0.81	0.62
Maximum Blast Pressure (GPa)	0.29	0.18	0.15

<sup>a</sup>The induced shock pressure ( $p_1$  in GPa) is related to the separation distance ( $r$  in mm) by  $p_1 = Ar^{-n}$ .

A	100	292	254
n	1.18	1.22	1.06

where the induced shock pressure  $p_1$  and the blast pressure  $p_B$  are in GPa. This relation is approximately valid for all three cube sizes within the limits of the data.

The effect of varying the length-to-diameter ratio,  $l/d$ , of the donor cylinder was determined from a study of calculated blast pressures. The pressures for two extreme values of  $l/d$  are shown in Fig. 13. These may be compared with the results for the simulated cube ( $l/d = 0.88$ ) shown in Fig. 11b. The calculations were made on cylinders with a constant length of 5.07 cm. The observed scaling with the cube root of the mass was applied to these data to obtain the variation of peak pressure with  $l/d$  for constant mass (mass of a 2-in. cube) shown in Fig. 14. If a minimum blast pressure of 0.18 GPa (calculated value for a 2-in. donor cube) is assumed to be necessary for the detonation of a 2-in. acceptor cube, then the critical separation distance is a maximum for  $l/d \sim 1$ , and decreases for any change of  $l/d$ . This observation ignores the effect of the duration of the detonation products shock pressure, however, and thus should be considered with caution.

The difference between end-on and side-on placement of the acceptor was also determined from a study of blast pressures. The calculated pressures in a direction parallel to the steel backing plate for the side-on case are shown in Fig. 15. These are compared with the pressures along the cylinder axis of the simulated cube for the end-on case in Fig. 16. The detonation products shock wave does not hit the side-on acceptor symmetrically, but the consequences of this effect are not known, and a calculation of this three-dimensional phenomenon is not possible with 2DE. The side-on blast wave is calculated also from the curved cylindrical face, rather than from a planar cube face. The exact calculation for the cube would also require a three-dimensional code. We can infer from Fig. 16, however, a critical separation distance of less than 2.5 cm for the side-on case of 2-in. cubes of VRO, compared with the calculated value of 3.63 cm for the end-on case.

#### IV. CONCLUSIONS

We have modeled successfully the sympathetic detonation of small cylindrical samples of rocket propellants using the 2DE code with Forest Fire burn rate. The results of the calculations are in very good agreement with experimental observations.

We can predict other results from a consideration of run distances, blast wave pressures, and induced pressures in the acceptor. The necessary condition for detonation of the acceptor cylinder is that the length of run to detonation be less than approximately 0.75 times the radius of

the acceptor. This run length is then converted to a necessary minimum induced pressure in the acceptor by means of the Pop plot. The blast pressure required to induce this pressure is obtained from

$$p_B = 0.02483 p_I^{3/2},$$

with the pressures in GPa. The distance from the donor at which this blast pressure will occur can be determined for VRO from the pressure vs distance plots of Figs. 12, 14, or 16. These pressure curves may be scaled by the cube root of the mass for different size donors. The variation of blast pressure for the different propellants is very small, and can probably be ignored. The effect of a different method of initiation of the donor cylinder, such as sympathetic detonation or flying plate impact, can be approximated by subtracting the length of run to detonation from the total length to obtain an effective length. This defines a different entry condition for the blast pressure curves.

Note that this model and the conclusions drawn from it apply only to single shock initiated detonations in the absence of any fragments.

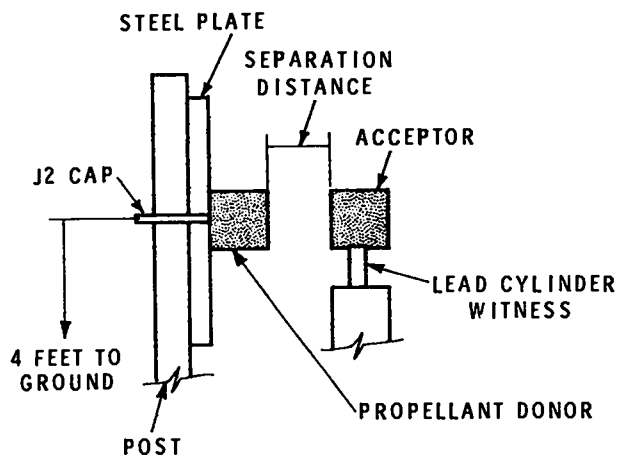


Fig. 1.  
Schematic test setup for sympathetic detonation experiment. (4 ft. = 1.2192 m.)

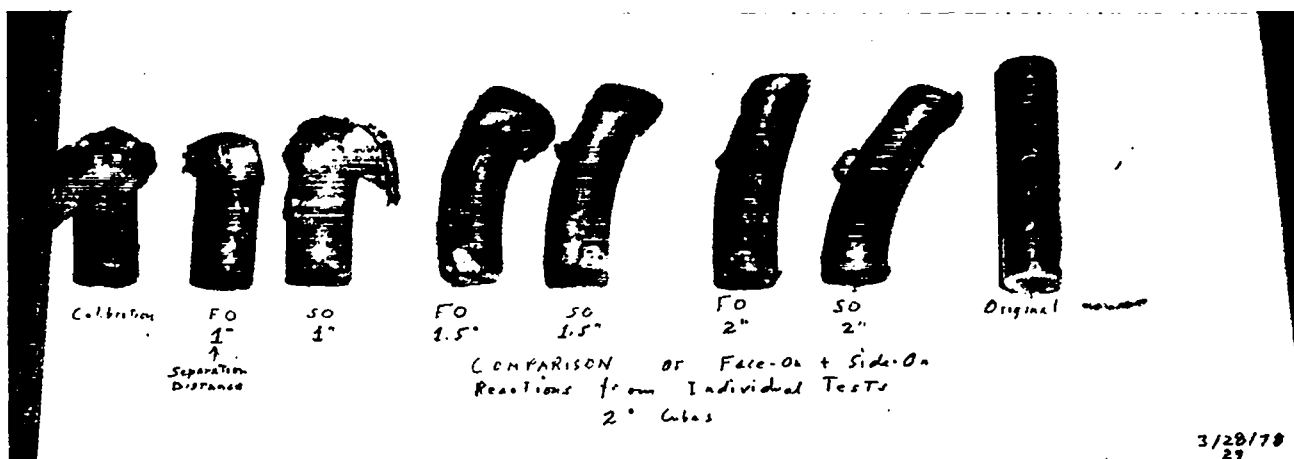


Fig. 2.

Lead witness cylinders from sympathetic detonation experiments, 2-in. cubes of VRO. Numbering from the left, 1 and 2 show a high-order detonation, 3 is marginal, 4-7 show the results of lesser reaction, and 8 is an original for comparison.

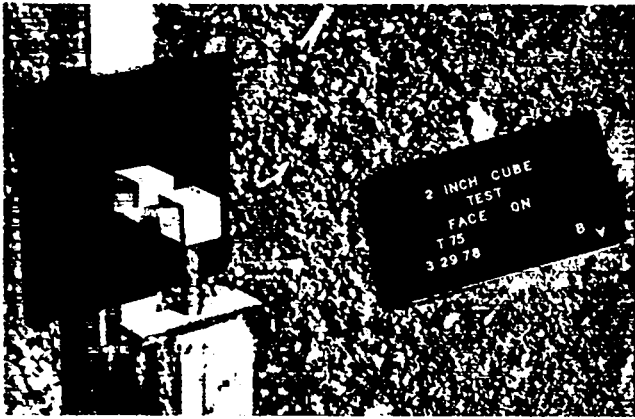
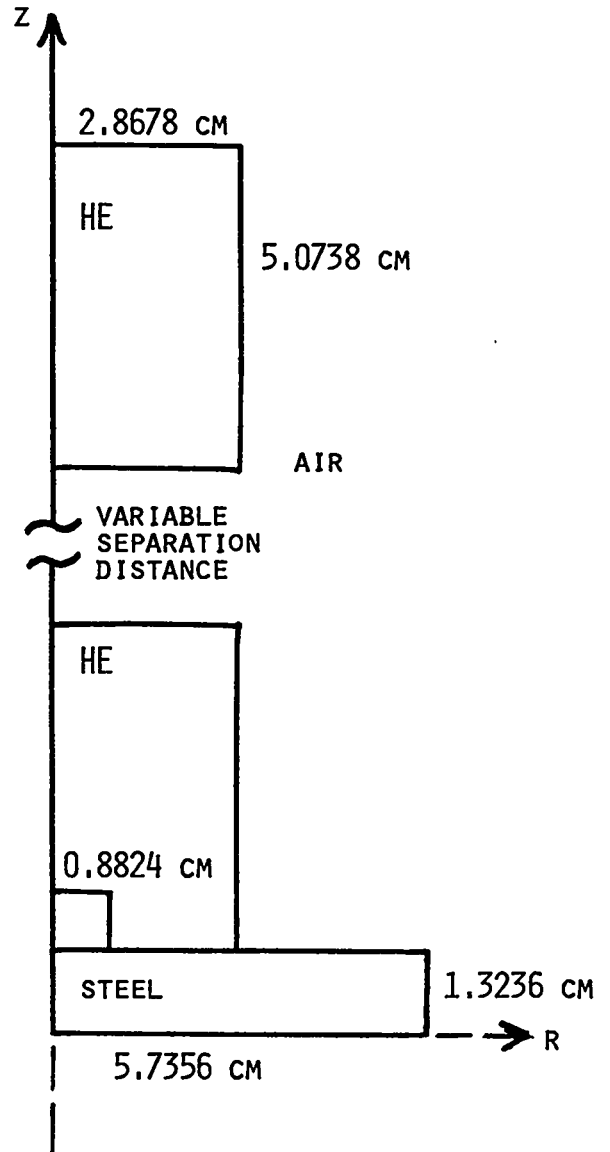


Fig. 4.  
Sympathetic detonation model, 2-in. cubes of high explosive (HE).

Fig. 3.  
Test setup for sympathetic detonation experiment.



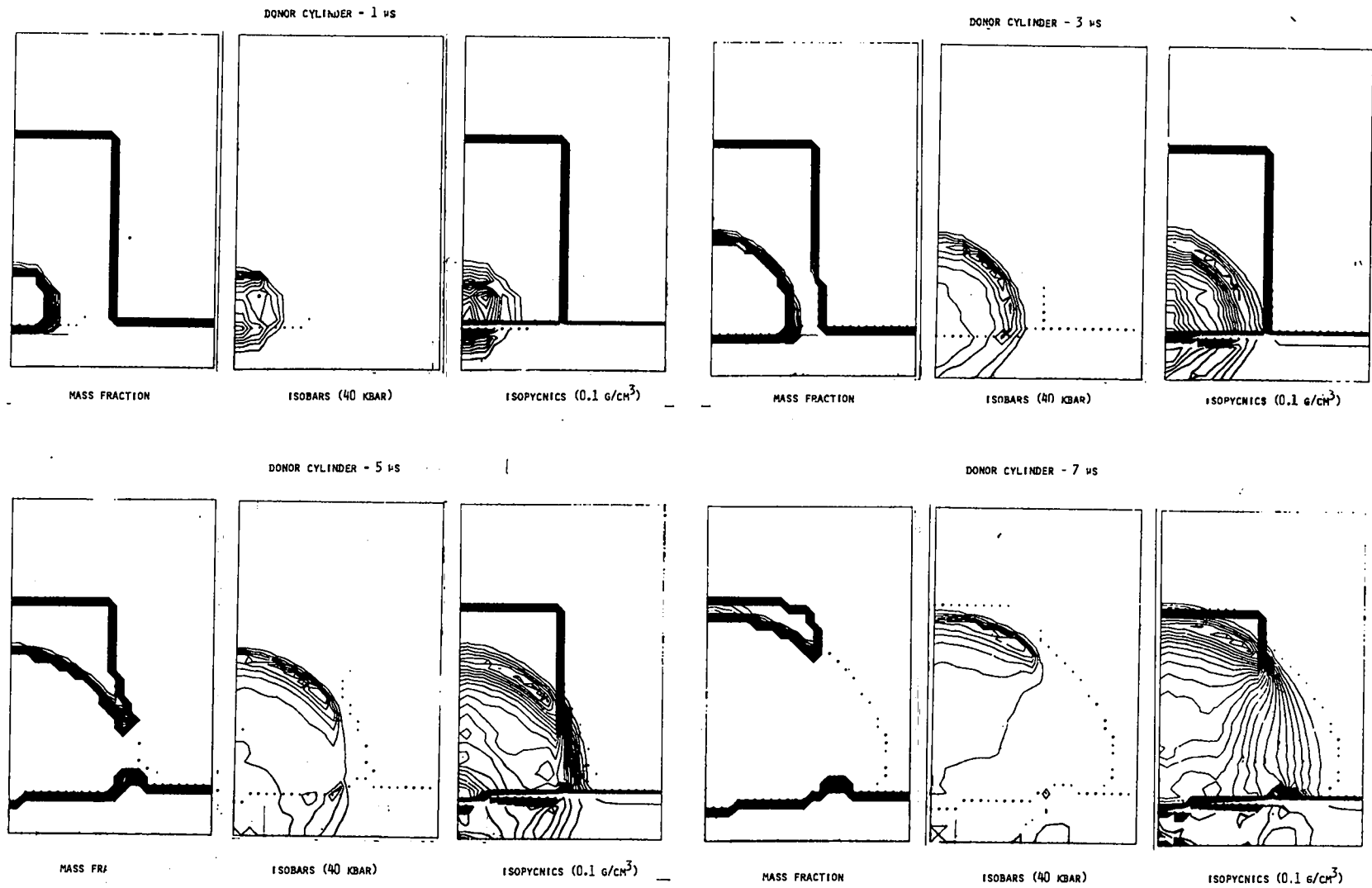


Fig. 5.  
 Detonation of the donor cylinder, VRO-simulated 2-in. cube at 1, 3, 5, and 7  $\mu$ s. Contour plots of mass fraction, pressure (40-kbar interval) and density (0.1-g/cm<sup>3</sup> interval).

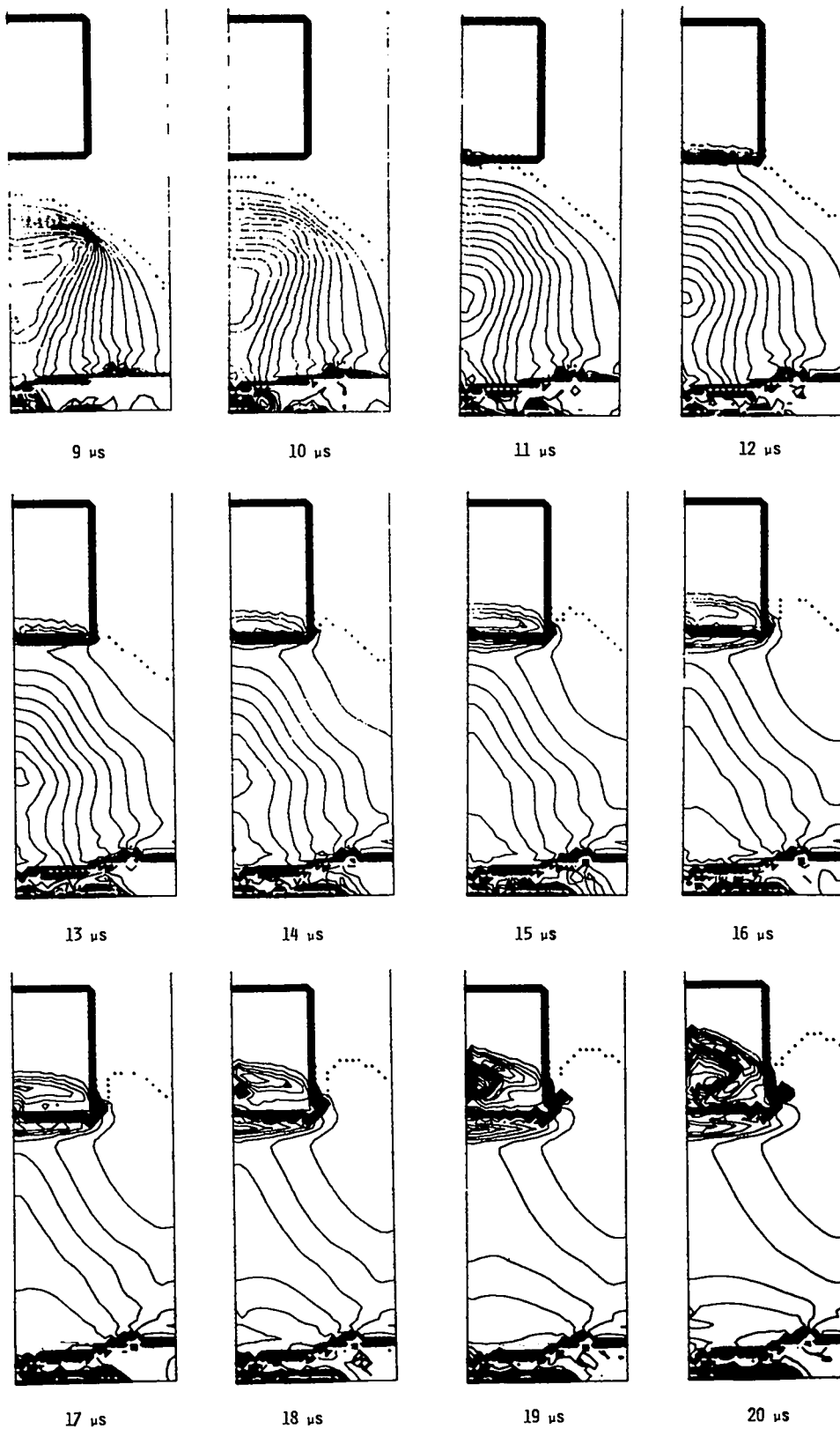
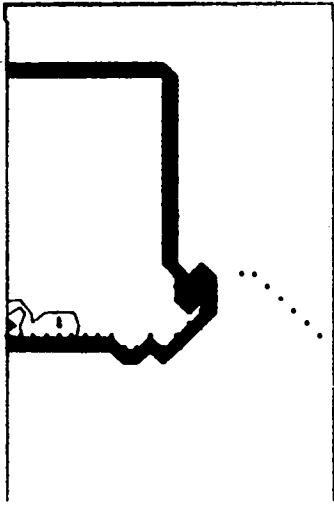
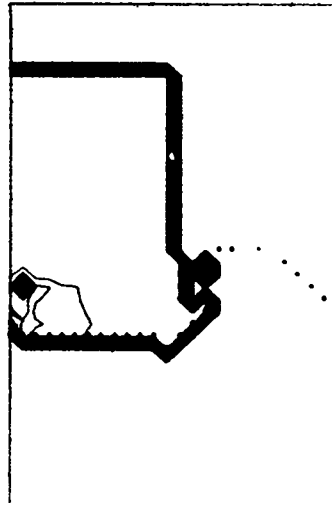


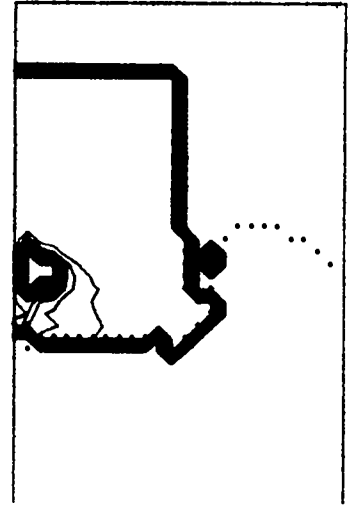
Fig. 6.  
 Blast wave in the air gap, VRO-simulated 2-in. cubes. Isopycnic contour plots (0.1-g/cm<sup>3</sup> interval).



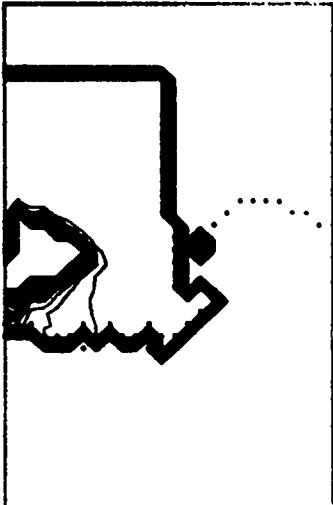
16  $\mu\text{s}$



17  $\mu\text{s}$



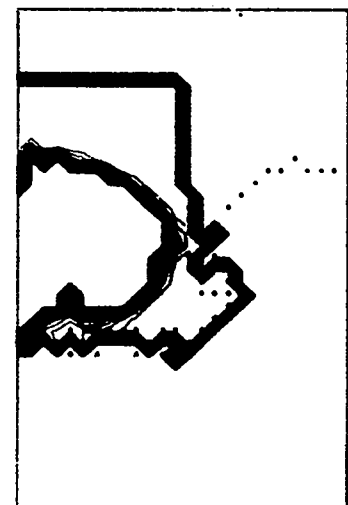
18  $\mu\text{s}$



19  $\mu\text{s}$



20  $\mu\text{s}$



21  $\mu\text{s}$

*Fig. 7.*

*Detonation in the acceptor cylinder, VRO-simulated 2-in. cubes with a 3.1-cm gap. Mass fraction contour plots.*

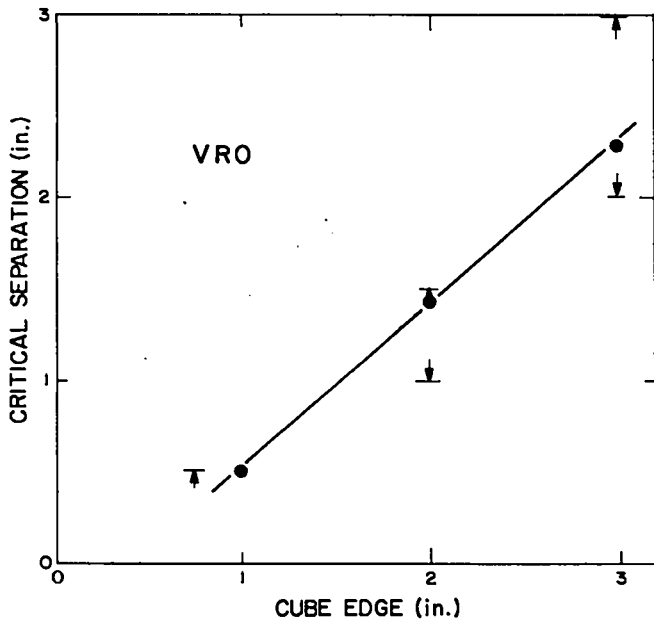


Fig. 8.

Variation of critical separation distance with cube size. Calculated values are shown by (●); experimental results are shown by arrows indicating the limits of observation.

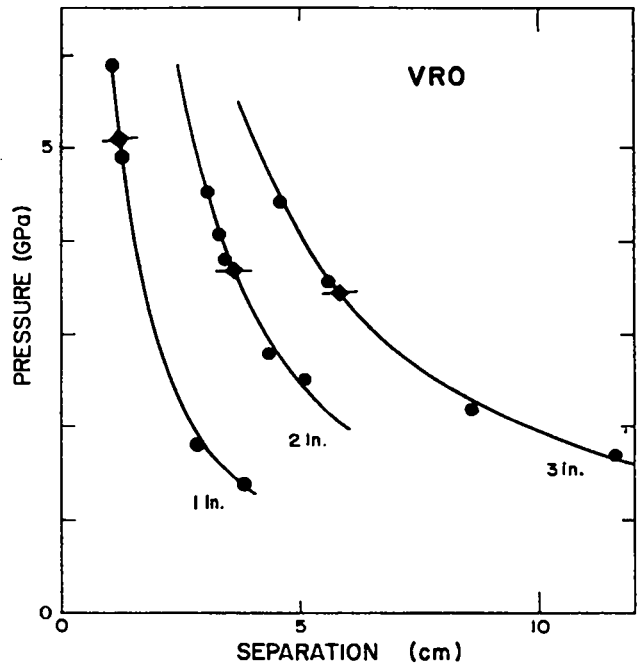


Fig. 9.

Variation of the maximum induced pressure in a nonreactive acceptor with separation distance. The critical separation distance is shown by (◆).

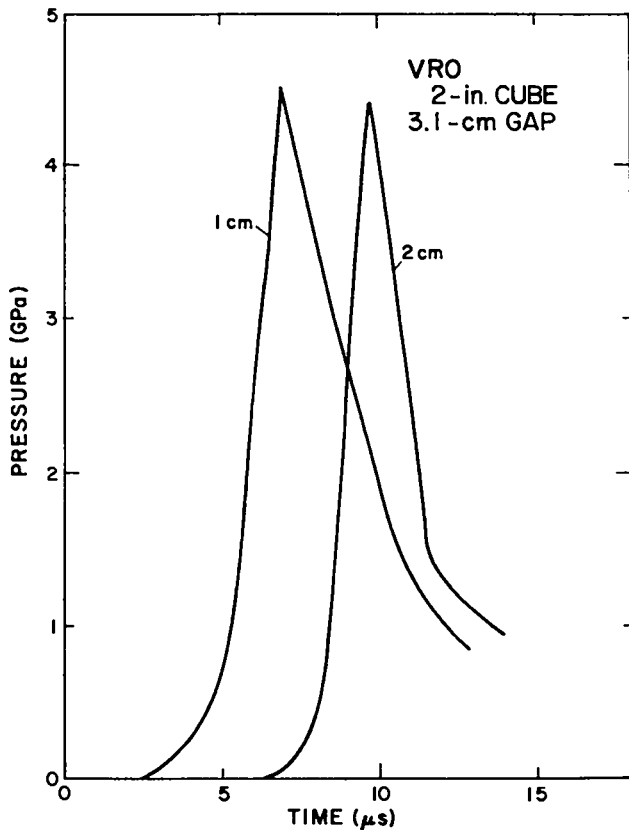


Fig. 10.

Shock-wave pressures induced in a nonreactive acceptor. Distances are measured from the front face.

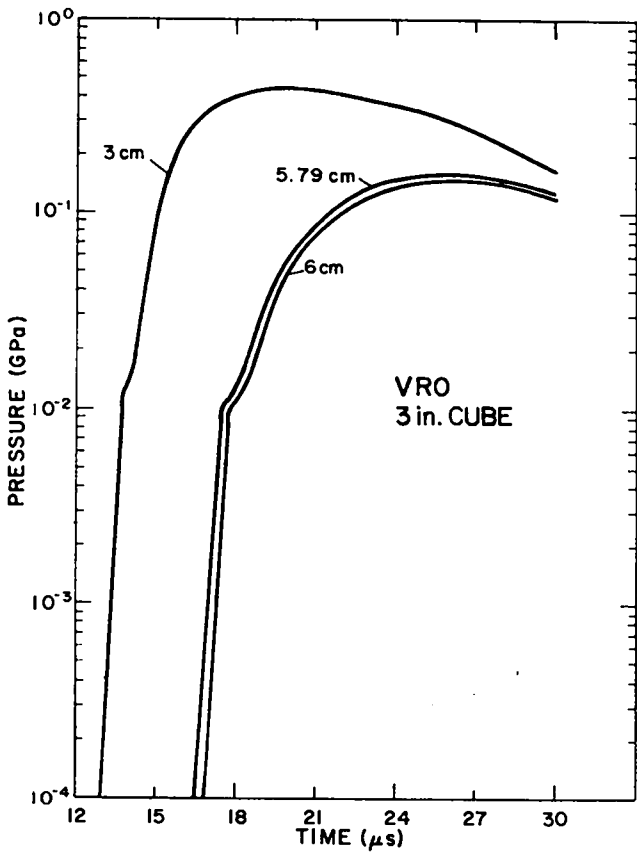
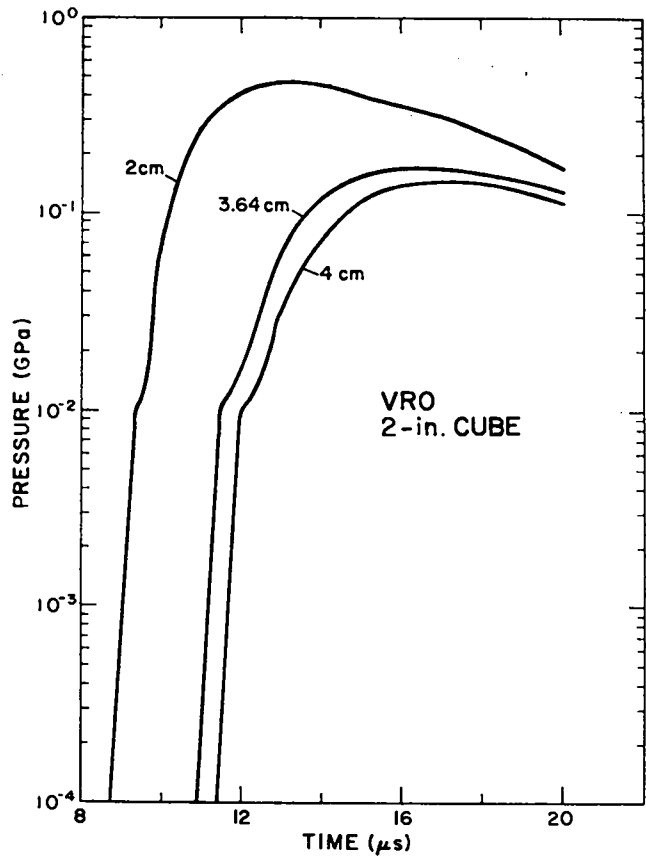
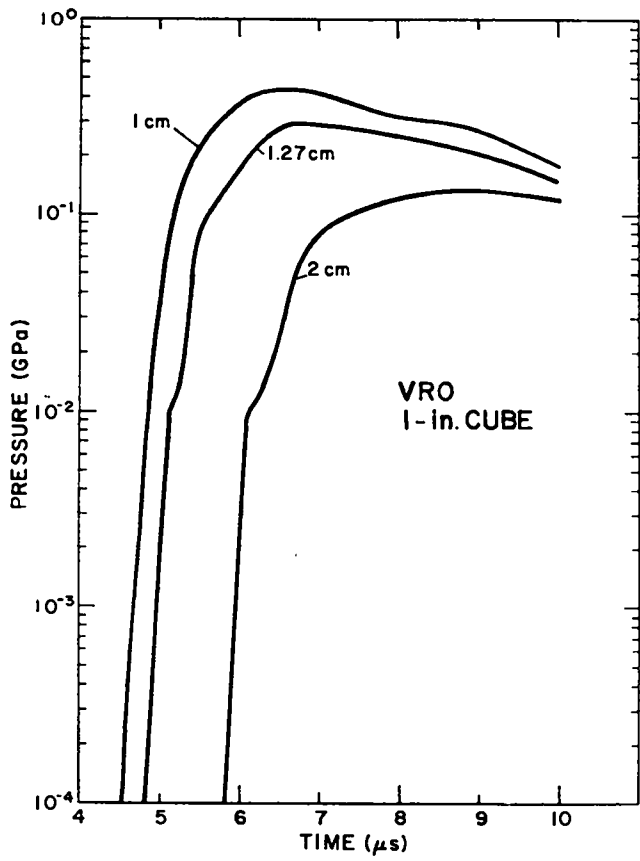


Fig. 11.  
Blast wave pressures in the air gap. The middle curve is at the critical separation distance.

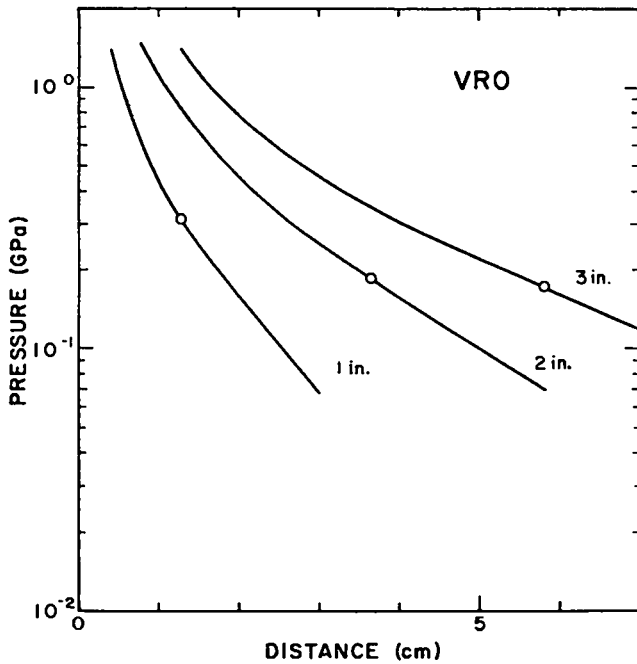


Fig. 12.  
Variation of peak blast pressure with distance from the donor for three cube sizes. The critical separation distance is shown by (o).

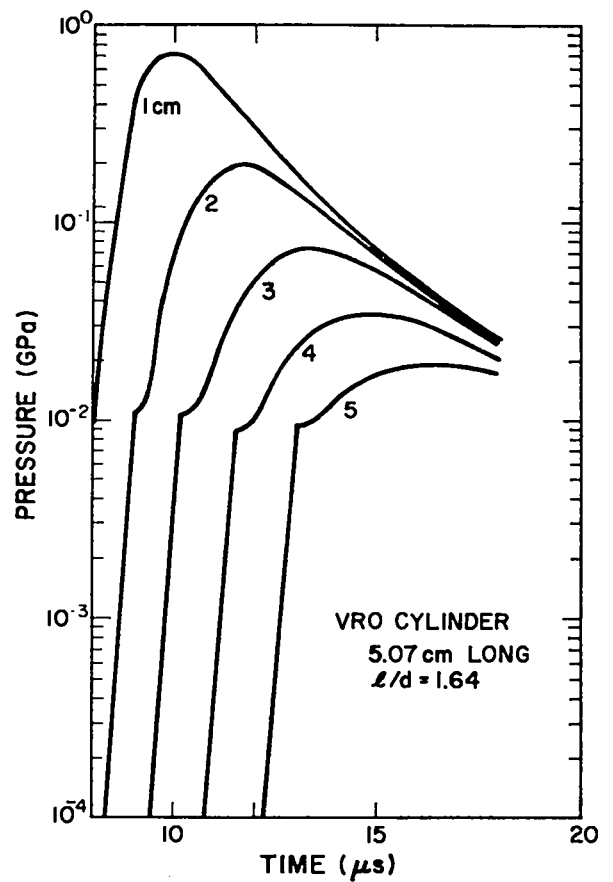
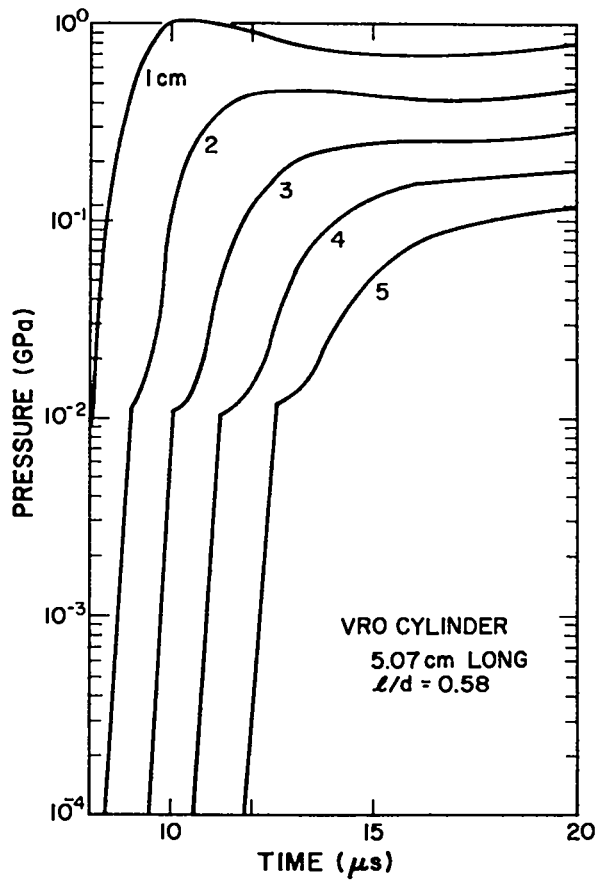


Fig. 13.  
Blast wave pressures in the air gap for different  $l/d$ .

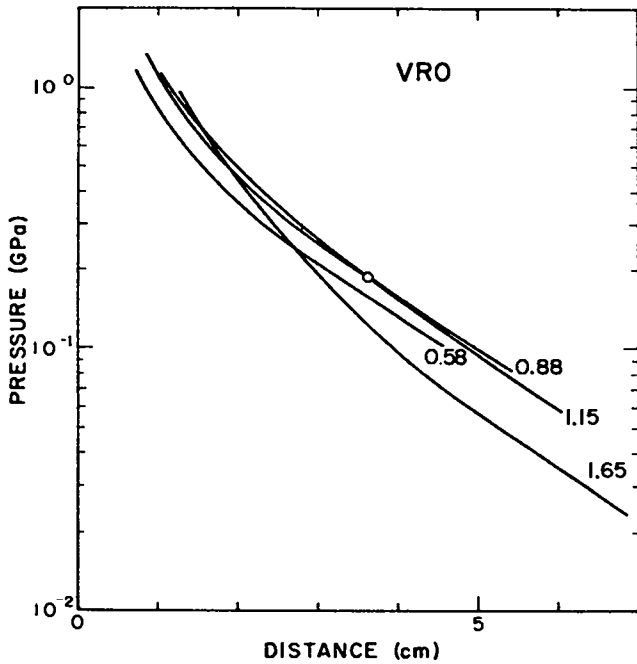


Fig. 14.  
 Variation of peak blast pressure with distance from the donor for cylinders of constant mass and different  $l/d$ . The critical separation distance for a 2-in. cube ( $l/d = 0.88$ ) is shown by (o).

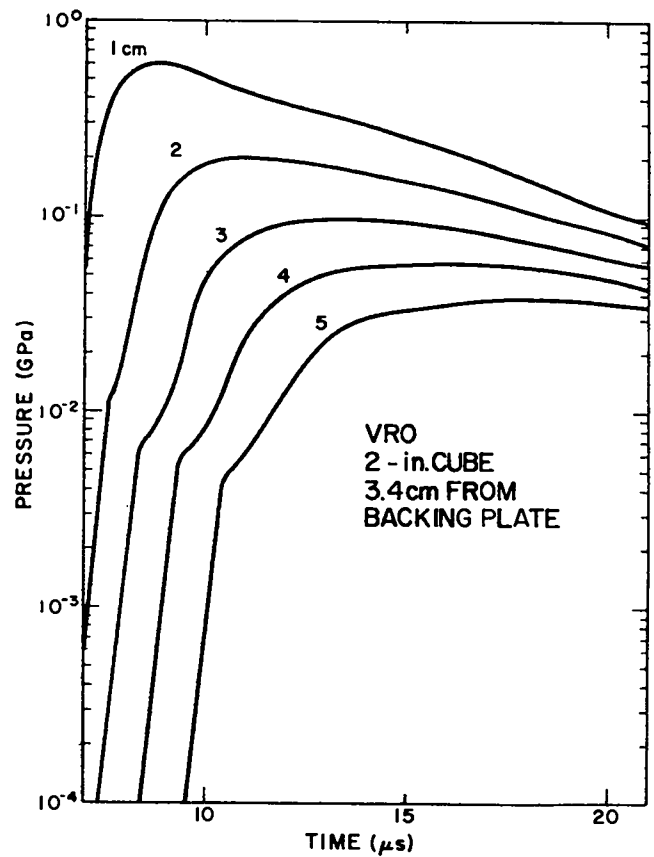
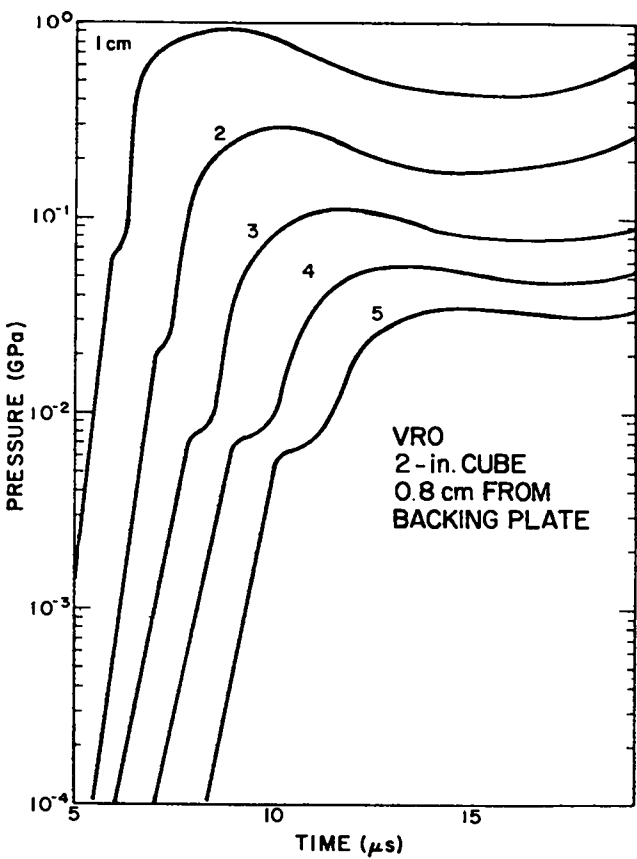


Fig. 15.  
 Blast wave pressures to the side of a simulated cube donor.

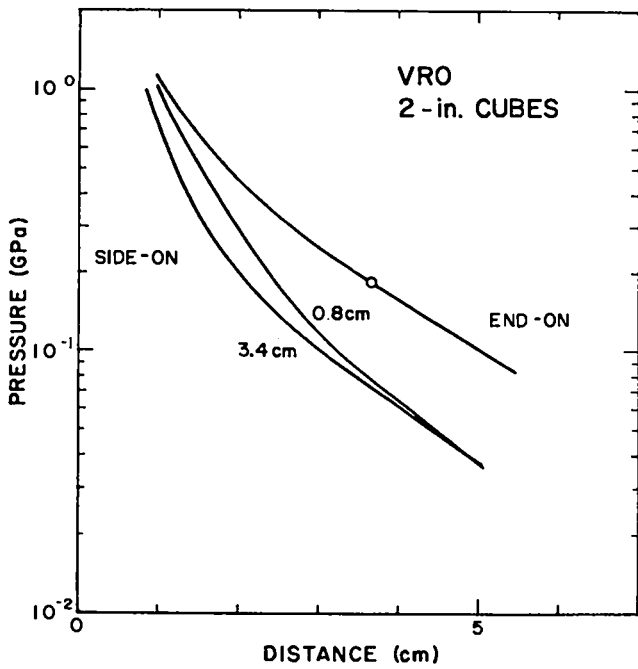
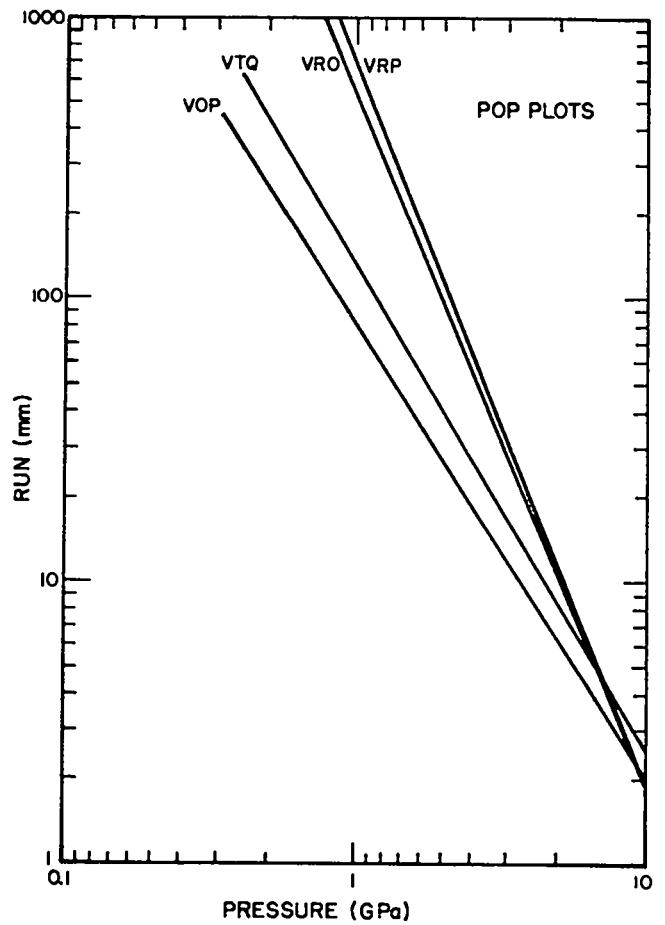


Fig. 16.  
Variation of peak blast pressure with distance from the donor for end-on and side-on cases. The side-on calculations are for two different distances from the steel plate. The calculated critical separation distance for the end-on case is shown by (o).

Fig. 17.  
Pop plots for the propellants of this study.



## APPENDIX A

### EQUATION OF STATE

The HOM equation of state is used to solve for pressure  $P$  and temperature  $T$  in a cell, with specific volume  $V$  and specific internal energy  $I$  as input. The shock velocity  $U_s$  and the particle velocity  $U_p$  are related by

$$U_s = C + S U_p .$$

The equations for a solid are

$$P_H = C^2(V_0 - V)/[V_0 - S(V_0 - V)]^2$$

$$X = \ln V$$

$$\ln T_H = F + GX + HX^2 + IX^3 + JX^4$$

$$I_H = (1/2) P_H(V_0 - V)$$

$$P = (\gamma/V) (I - I_H) + P_H$$

$$T = (I - I_H) (23\ 890)/C_v + T_H$$

The equations for a gas are

$$X = \ln V$$

$$Y = \ln P_1$$

$$Y = A + BX + CX^2 + DX^3 + EX^4$$

$$\ln I_1 = K + LY + MY^2 + NY^3 + OY^4$$

$$I_1 = I_1 - Z$$

$$\ln T_1 = Q + RX + SX^2 + TX^3 + UX^4$$

$$-1/\beta = R + 2SX + 3TX^2 + 4UX^3$$

$$P = [1/(\beta V)] (I - I_1) + P_1$$

$$T = (I - I_1) (23\ 890)/C_v + T_1$$

The solution for a cell with more than one component is based on combinations of these equations.<sup>1,2</sup>

The equation-of-state parameters used in this study are tabulated in Table A-I. The units are volume ( $\text{cm}^3/\text{g}$ ), energy ( $\text{Mbar}\cdot\text{cm}^3/\text{g}$ ), pressure (Mbar), temperature (K), velocity ( $\text{cm}/\mu\text{s}$ ), and heat capacity ( $\text{cal}/\text{g}\cdot\text{K}$ ).

TABLE A-I

EQUATION OF STATE PARAMETERS

VRO

C	1.95500000000E-01	D	-3.99000528800E-02
S	2.20000000000E+00	E	1.92083720688E-03
F	5.99972212685E-01	K	-1.56422272062E+00
G	-1.42854580100E+01	L	5.23937060075E-01
H	-1.55490810707E+00	M	7.25982854693E-02
I	2.49789886336E+01	N	5.28235988917E-03
J	1.90620913522E+01	O	1.43028333133E-04
	1.50000000000E+00	Q	7.94579701924E+00
C	3.30000000000E-01	R	-4.67757303585E-01
V	5.45553737043E-01	S	1.18796956051E-01
	1.83500000000E-04	T	-1.73023803935E-02
A	-3.58530792618E+00	U	9.31272114867E-04
B	-2.29024912291E+00	C'	5.00000000000E-01
C	3.16804501752E-01	Z	1.00000000000E-01

VRP

C	1.99000000000E-01	D	-3.94574700710E-02
S	2.00000000000E+00	E	1.86437978542E-03
F	-5.40502394255E+00	K	-1.57124113947E+00
G	-4.86025889997E+01	L	5.35136520243E-01
H	-7.54072015339E+01	M	7.67136706803E-02
I	-4.56992180220E+01	N	5.76342096779E-03
J	-6.62503957745E+00	O	1.60356885887E-04
	1.50000000000E+00	Q	7.96340485711E+00
C	3.00000000000E-01	R	-4.82226700328E-01
V	5.44662309368E-01	S	1.20767297198E-01
	1.63000000000E-04	T	-1.70230990191E-02
A	-3.56380388220E+00	U	8.86138770815E-04
B	-2.30435144510E+00	C'	5.00000000000E-01
C	3.18097259766E-01	Z	1.00000000000E-01

VTQ

C	1.98000000000E-01	D	-3.84065208171E-02
S	2.23000000000E+00	E	1.81393039475E-03
F	5.82606573241E-01	K	-1.56687680661E+00
G	-1.30770444275E+01	L	5.28664483962E-01
H	3.05673979749E+00	M	7.30767018647E-02
I	3.06801060993E+01	N	5.30349447649E-03
J	2.13250350559E+01	O	1.43461617399E-04
	1.50000000000E+00	Q	7.92725310775E+00
C	3.30000000000E-01	R	-4.74542294271E-01
V	5.39956803456E-01	S	1.20944307504E-01
	1.76000000000E-04	T	-1.74893025065E-02
A	-3.58647450079E+00	U	9.33356217842E-04
B	-2.29146630829E+00	C'	5.00000000000E-01
C	3.11339201717E-01	Z	1.00000000000E-01

TABLE A-I (cont)

VOP

C	2.43000000000E-01	D	-3.38388105820E-02
S	1.87900000000E+00	E	3.26317134386E-04
F	-1.31440849980E+01	K	-1.56957579960E+00
G	-8.52022804900E+01	L	5.63240444400E-01
H	-1.41271692413E+02	M	9.14476859530E-02
I	-9.96282582660E+01	N	8.61048912340E-03
J	-2.35782395000E+01	O	3.20340178820E-04
	1.50000000000E+00	Q	8.05038175420E+00
C	3.30000000000E-01	R	-4.75298681100E-01
V	5.23560209424E-01	S	1.00767476473E-01
	1.16965000000E-04	T	5.25836857190E-03
A	-3.59225007104E+00	U	-4.21628859200E-03
B	-2.25139095825E+00	C'	5.00000000000E-01
C	3.07083271071E-01	Z	1.00000000000E-01

Steel

C	4.58000000000E-01	J	-1.66391615983E+03
S	1.51000000000E+00		2.00000000000E+00
F	-3.82382587453E+03	C	1.07000000000E-01
G	-7.03211954024E+03	V	1.26310471100E-01
H	-4.82670213890E+03		1.17000000000E-05
I	-1.46678402118E+03		

Air

A	-4.50602542688E+00	D	-1.58521895338E-06
B	-1.27546110628E+00	Q	8.22644581441E+00
C	-3.74276600292E-03	R	-2.51525130950E-01
D	1.23929236747E-02	S	-1.34446940047E-02
E	-2.07694122929E-03	T	1.40871016422E-02
K	-1.62655447438E+00	U	-2.18132189985E-03
L	9.05283146618E-02	C'	5.00000000000E-01
M	2.69004997726E-03	Z	1.00000000000E-01
N	-5.43583122192E-05	V	8.65224000000E+02

## APPENDIX B

### FOREST FIRE BURN RATE

The mass fraction of unburned explosive  $W$  is defined as  $W = 1$  for pure solid, and burns to gaseous products,  $W = 0$ , according to a pressure-dependent rate law based on experimental data.<sup>2,3</sup> The rate  $R$  is defined for pressure  $P$  in Mbars and time  $t$  in  $\mu s$  by

$$R = (1/W) (dW/dt) ,$$

$$\ln R = \sum_{i=1}^N C_i P^{i-1} .$$

The limiting conditions set  $R = 0$  for  $P$  less than a specified cutoff pressure and  $R = \infty$  ( $W \rightarrow 0$  immediately) when  $P$  reaches the C-J pressure. The rate parameters used in this study are tabulated in Table B-I.

TABLE B-I

#### FOREST FIRE RATE PARAMETERS

##### VRO

C-J PRESSURE = .292

CUT-OFF PRESSURE = .003

C(I=1,15) = -1.56083247170E+01	1.10033387470E+03	-6.38450445280E+04
2.56319147400E+06	-6.86159425460E+07	1.25930251590E+09
-1.62792529730E+10	1.51053650060E+11	-1.01596964460E+12
4.95447961760E+12	-1.73271008470E+13	4.23221598690E+13
-6.85089273350E+13	6.60059788540E+13	-2.86405109130E+13

##### VRP

C-J PRESSURE = .296

CUT-OFF PRESSURE = .003

C(I=1,13) = -1.19363902480E+01	3.45272091460E+02	-3.85251737840E+03
-6.46454623070E+04	3.46658142630E+06	-6.61456246930E+07
7.43123174580E+08	-5.43166919100E+09	2.65689688720E+10
-8.64258641880E+10	1.79559239130E+11	-2.15698911880E+11
1.14003029800E+11		

##### VTQ

C-J PRESSURE = .302

CUT-OFF PRESSURE = .003

C(I=1,15) = -1.28314444110E+01	9.65846203640E+02	-6.11854737060E+04
2.67124416920E+06	-7.74855482010E+07	1.53728164880E+09
-2.14475562680E+10	2.14534045230E+11	-1.55419284210E+12
8.15848111090E+12	-3.06982830050E+13	8.06429562810E+13
-1.40352955990E+14	1.45352577420E+14	-6.77786939670E+13

TABLE B-I (cont)

VOP

C-J PRESSURE = .318

CUT-OFF PRESSURE = .003

c(I=1,15) =	-1.20404002280E+01	9.08756994130E+02	-5.42153602360E+04
	2.14408315320E+06	-5.50111899880E+07	9.50651793330E+08
	-1.14326788170E+10	9.78377619830E+10	-6.02953546360E+11
	2.68033534670E+12	-8.50846157910E+12	1.87941446800E+13
	-2.74209509530E+13	2.37376212750E+13	-9.22624218830E+12

These Forest Fire parameters are derived from the experimentally determined Pop plots. The equation of the Pop plot is

$$\ln x = A + B \ln P ,$$

with the run distance x in cm and the pressure P in Mbars. The Pop plots are shown in Fig. 17. The parameters are given in Table B-II.

TABLE B-II

POP PLOT PARAMETERS

	<u>A</u>	<u>B</u>
VRO	-7.20628	-2.43068
VRP	-7.520548	-2.550833
VTQ	-5.263	-1.706
VOP	-5.299277	-1.613201

REFERENCES

1. J. D. Kershner and C. L. Mader, "2DE, A Two-Dimensional Continuous Eulerian Hydrodynamic Code for Computing Multicomponent Reactive Hydrodynamic Problems," Los Alamos Scientific Laboratory report LA-4846 (March 1972).
2. C. L. Mader, *Numerical Modeling of Detonations* (University of California Press, Berkeley, 1979).
3. C. L. Mader and C. A. Forest, "Two-Dimensional Homogeneous and Heterogeneous Detonation Wave Propagations," Los Alamos Scientific Laboratory report LA-6259 (June 1976).
4. C. L. Mader, "FORTRAN BKW: A Code for Computing the Detonation Properties of Explosives," Los Alamos Scientific Laboratory report LA-3704 (July 1967).

Printed in the United States of America. Available from  
National Technical Information Service  
US Department of Commerce  
5285 Port Royal Road  
Springfield, VA 22161

Microfiche \$3.00

001-025	4.00	126-150	7.25	251-275	10.75	376-400	13.00	501-525	15.25
026-050	4.50	151-175	8.00	276-300	11.00	401-425	13.25	526-550	15.50
051-075	5.25	176-200	9.00	301-325	11.75	426-450	14.00	551-575	16.25
076-100	6.00	201-225	9.25	326-350	12.00	451-475	14.50	576-600	16.50
101-125	6.50	226-250	9.50	351-375	12.50	476-500	15.00	601-up	

Note: Add \$2.50 for each additional 100-page increment from 601 pages up.